Modification of structural disorder by hydrostatic pressure in the superconducting cuprate $YBa_2Cu_3O_{6.73}$

H. Huang,[1,2,3] H. Jang,[1,*] M. Fujita,[4] T. Nishizaki,[5] Y. Lin,[6] J. Wang,[2,3] J. Ying,[7] J. S. Smith,[7] C. Kenney-Benson,[7] G. Shen,[7] W. L. Mao,[6,8] C.-C. Kao,[9] Y.-J. Liu,[1,†] and J.-S. Lee[1]

[1]*Stanford Synchrotron Radiation Lightsource, SLAC National Accelerator Laboratory, Menlo Park, California 94025, USA*
[2]*State Key Laboratory of Infrared Physics, Shanghai Institute of Technical Physics, Chinese Academy of Sciences, Shanghai 200083, China*
[3]*University of Chinese Academy of Sciences, Beijing 100049, China*
[4]*Institute for Materials Research, Tohoku University, Katahira 2-1-1, Sendai, 980-8577, Japan*
[5]*Department of Electrical Engineering, Kyushu Sangyo University, Fukuoka 813-8503, Japan*
[6]*Stanford Institute for Materials and Energy Sciences, SLAC National Accelerator Laboratory, Menlo Park, California 94025, USA*
[7]*High Pressure Collaborative Access Team, Geophysical Laboratory, Carnegie Institution of Washington, Argonne, Illinois 60439, USA*
[8]*Geological Sciences, Stanford University, Stanford, California 94305, USA*
[9]*SLAC National Accelerator Laboratory, Menlo Park, California 94025, USA*

(Received 18 September 2017; revised manuscript received 16 April 2018; published 9 May 2018)

Compelling efforts to improve the critical temperature (T_c) of superconductors have been made through high-pressure application. Understanding the underlying mechanism behind such improvements is critically important; however, much remains unclear. Here we studied ortho-III $YBa_2Cu_3O_{6.73}$ (YBCO) using x-ray scattering under hydrostatic pressure (HP) up to ~6.0 GPa. We found the reinforced oxygen order of YBCO under HP, revealing an oxygen rearrangement in the Cu-O layer, which evidently shows the charge-transfer phenomenon between the CuO_2 plane and Cu-O layer. Concurrently, we also observed no disorder-pinned charge-density-wave signature in CuO_2 plane under HP. This indicates that the oxygen rearrangement modifies the quenched disorder state in the CuO_2 plane. Using these results, we appropriately explain why pressure condition can achieve higher T_c compared with the optimal T_c under ambient pressure in $YBa_2Cu_3O_{6+x}$. As an implication of these results, finally we have discussed that the change in disorder could make it easier for $YBa_2Cu_3O_{6+x}$ to undergo a transition to the nematic order under an external magnetic field.

DOI: 10.1103/PhysRevB.97.174508

I. INTRODUCTION

Since high-temperature superconductivity (HTSC) in La-based cuprate was discovered in 1986 [1], cuprates have been a significant focus of the HTSC research activities aiming for further improvement in T_c [2–5]. The highest reported T_c at ambient pressure is 134 K in Hg-based cuprate [6]. Meantime, the current record-setting T_c at 203 K in the sulfur-hydride system was recently reported under high-pressure application [7]. Indeed, pressure-induced T_c changes have also been reported in many cuprates [8–12]. For example, the Hg-based cuprate, $HgBa_2Ca_2Cu_3O_{8+\delta}$, shows T_c increase up to 164 K at 31 GPa [9]. In $YBa_2Cu_4O_8$ ($T_c = 80$ K at ambient pressure), T_c increases up to 108 K at 10 GPa [10]. Therefore, concurrent with efforts that survey a large number of materials in varying compositions, applying high pressure to the superconducting materials has emerged as a promising approach that can efficiently improve superconductivity. Nevertheless, "why does T_c change upon compression?" is an essential and fundamental question that still needs to be addressed.

Archetypal Y-based cuprate, $YBa_2Cu_3O_{6+x}$, has been the active subject of many high-pressure HTSC investigations in both experiments [11–18] and theories [14,19–23], aiming to address this question. This is in part due to $YBa_2Cu_3O_{6+x}$ being widely appreciated as one of the cleanest cuprates [24–26]. Figure 1(a) represents the T_c behavior for $YBa_2Cu_3O_{6+x}$ without and with high pressure ($P = 0$ and $P > 0$, respectively) [11–17,27]. The T_c is increased up to the optimal doping (where $p \sim 0.165$, $x \sim 0.91$) upon compression. Above the optimal doping range, compression reduces the T_c. According to the previous reports [13,14,27], such T_c change has been mainly attributed to the change in bonding lengths along the c axis, in particular, the distance between the Cu-O chain layer and CuO_2 plane [Fig. 1(b)]. Compression brings the Cu-O chain layer closer to the CuO_2 plane, which enhances charge transfer between the planes, leading to additional hole doping in the CuO_2 plane, as theoretically explained [14,20–23]. In this context, the decrement of T_c in the overdoped regime (i.e., $dT_c/dP < 0$) is well explained by the increment of hole doping through external pressure [11,12]. In addition, the in-plane oxygen movement in the structurally disordered Cu-O chain layer is considered as an additional hole-doping source into the CuO_2 plane. Simultaneously, such compression-induced oxygen movement modifies the oxygen order in YBCO [14–16,18,23,28]. However, this hypothesis is not fully established yet, due to the absence of direct

*Present address: PAL-XFEL Beamline Division, Pohang Accelerator Laboratory, 80 Jigokro-127-beongil, Nam-gu, Pohang, Gyeongbuk 37673, Republic of Korea; h.jang@postech.ac.kr
†liuyijin@slac.stanford.edu

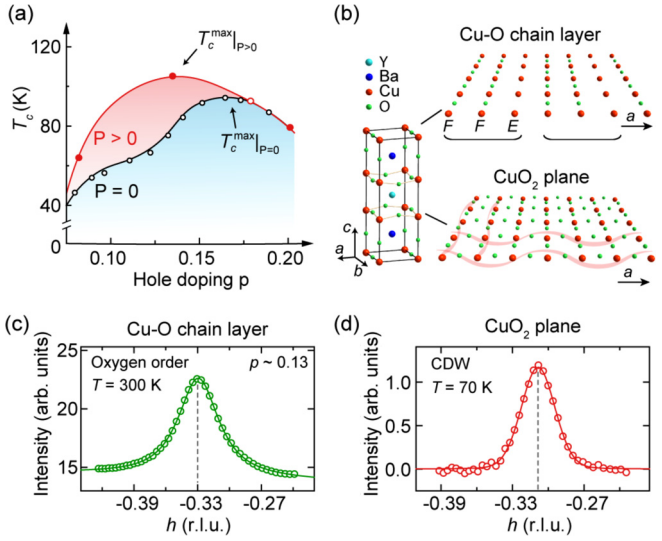

FIG. 1. (a) T_c phase diagram of YBCO with/without the high pressure. The arrows indicate the optimal T_c values. The black circles denote ambient pressure data [27]. Red-colored filled (opened) circles are at 15 GPa (2 GPa) [12,17]. (b) The crystal structure of YBCO (left) and extended drawings of the Cu-O chain layer with the oxygen order and CuO_2 plane with CDW. (c), (d) RSXS data—-ortho-III oxygen order and CDW—-measured at 933.7 and 930.8 eV, respectively. Dashed lines indicate peak positions of the oxygen order (at $h = -0.33$ r.l.u.) and CDW (at $h = -0.31$ r.l.u.). Solid lines are curves fitted to the data.

experimental evidence. Moreover, the reported maximum T_c under high pressure ($T_c^{\max}|_{P>0} \sim 107$ K in $YBa_2Cu_3O_{6.66}$ and $p \sim 0.134$) [12,17] is considerably higher than that under ambient pressure ($T_c^{\max}|_{P=0} \sim 94$ K) [27]. This indicates that charge-transfer mechanism (i.e., doping change) is unlikely the sole reason for the pressure-induced T_c improvement. This is because, if the change in T_c upon compression is only driven by the doping, the $T_c^{\max}|_{P>0}$ must be the same as, or at least similar to, the $T_c^{\max}|_{P=0}$. In this context, a charge-density-wave (CDW) within the CuO_2 planes, which is competing with YBCO's superconductivity [29–39] and understood as the reason of the T_c plateau around $p \sim 1/8$ [29–31,34,39], has been recently proposed as an additional driving force for the T_c change under high pressure [17]. In addition, the pressure-induced T_c change would be associated with the magnetic interactions between Cu spins, which are ultimately responsible for the superconducting mechanism in cuprates, expecting that this may be revealed through the observation of the change of excitation spectrum by inelastic neutron- or x-ray scattering experiments under high pressure [40,41]. However, there is a lack of evidence to support these proposals. As a result, we are still in early stages of understanding the underlying mechanism(s) for the pressure-induced T_c changes.

In this work, we performed x-ray scattering measurements on an underdoped $YBa_2Cu_3O_{6.73}$ ortho-III crystal ($p \sim 0.13$, $T_c \sim 70$ K). We observed that the pressure modifies the disorder state in YBCO, leading to an enhancement of oxygen ordering in the Cu-O layer and a suppression of disorder-pinned CDW fluctuations in the CuO_2 plane. Through these results, we could verify the role of the structural disorder. Finally, we understand the reason why pressure can increase the T_c in $YBa_2Cu_3O_{6+x}$ to a level that is considerably higher than the optimal T_c under ambient pressure.

II. EXPERIMENTAL DETAILS

High-quality single crystals of $YBa_2Cu_3O_{6.73}$ were grown by self-flux method using Y_2O_3 crucible [42,43]. The oxygen content (x) was controlled by the annealing condition under oxygen flow atmosphere. The superconducting transition temperature T_c was determined by the magnetization measurements using a superconducting quantum interference device magnetometer (MPMS3). The measured YBCO crystals annealed at 630 °C for 7 days show sharp superconducting transitions with $T_c \sim 70$ K. Since this single crystal prepared by the same method shows the first-order vortex lattice melting transition and sharp diffraction peaks, the single crystals studied in this work are clean and highly crystalline. The crystal was a twinned sample but twinned domains could be easily distinguishable by x-ray diffraction. It is because the lattice parameters a and b are quite different [more than 1%, Fig. 2(c)] and the oxygen-order wave vector is only along the h direction.

For this study, we employed two scattering approaches: resonant soft x-ray scattering (RSXS) and high-pressure hard x-ray diffraction. First, the RSXS experiments were performed at beamline 13-3 of the Stanford Synchrotron Radiation Lightsource (SSRL). The *ex situ* cleaved YBCO crystal was mounted on an in-vacuum four-circle diffractometer and cooled down with an open-flow liquid helium cryostat. (h, 0, l) scattering plane was explored by rotating sample angle (θ) after aligning the crystalline ac plane parallel to the scattering plane. A

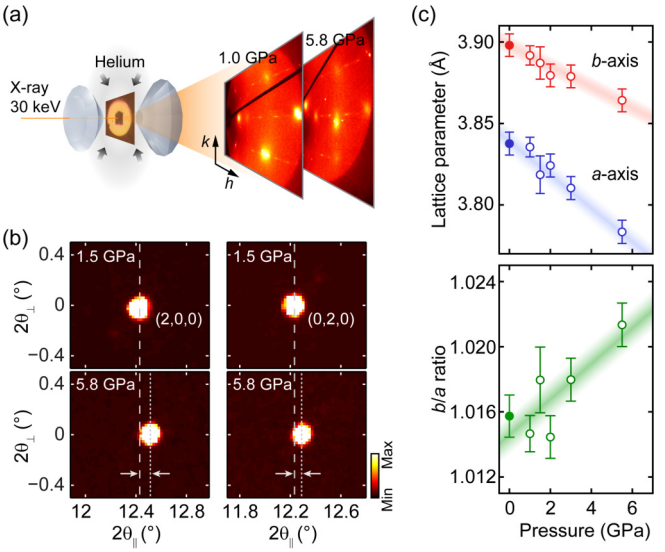

FIG. 2. (a) Transmission geometry for x-ray diffraction at hydrostatic high pressure. Images show 2D diffraction patterns obtained at 1.0 and 5.8 GPa. Black lines on diffraction patterns are the shadows of the beamstop. (b) Zoomed images of lattice peaks −(2, 0, 0) and (0, 2, 0). Dashed and dotted lines denote positions of $2\theta_{\parallel}$ at 1.5 and 5.8 GPa, respectively. (c) Pressure-dependent a- and b-axis lattice parameters (upper panel) and b/a ratio, i.e., orthorhombicity (lower). Note that data at $P = 0$ (closed circles) are obtained from the RSXS. Error bars correspond to 1 standard deviation.

two-dimensional charge-coupled device (CCD) detector was utilized to detect a diffraction pattern over a wide reciprocal space. The center of the CCD was fixed at the scattering angle, $2\theta = 156^\circ$. Because of the quasi-2D nature of the oxygen order and CDW [34,44], the peaks are observed in broad l range, and the value ($l = \sim 1.4$ in the current experiment) is determined by the 2θ position. The photon polarization was perpendicular to the scattering plane (σ polarization), which ensures strong signal for both the oxygen order and CDW [31]. Second, the high-pressure hard x-ray diffraction experiments were performed at beamlines 16-ID-B and 16-BM-D of the Advanced Photon Source (APS). The YBCO single crystal with dimensions of $a \times b \times c \approx 80 \times 60 \times 40\,\mu\text{m}^3$ was mounted in the diamond-anvil cell (DAC) with compressed helium gas loaded as the pressure medium to ensure the hydrostatic pressure environment up to our maximum pressure [45]. The DAC system was also installed on the open-circle cryostat, aiming for detecting a CDW signal around T_c. The 30-keV, high-energy x-ray, and a large 2D area detector were utilized to ensure that the hk-diffraction pattern could capture many of the lattice Bragg peaks, as well as the oxygen-order patterns.

III. X-RAY SCATTERING RESULTS AND DISCUSSION

In $YBa_2Cu_3O_{6+x}$, structural properties such as oxygen order and CDW have been widely appreciated as important ingredients for understanding its superconductivity. As a first step, we investigated these properties at ambient pressure in YBCO using the Cu L_3-edge RSXS. In the ideal ortho-III structure in YBCO, two fully filled (F) Cu-O chains and an oxygen-empty (E) Cu line along the crystalline b axis in the Cu-O chain layer show a periodic formation along the a axis: i.e., F-F-E-F-F-E-F … sequence [Fig. 1(b), upper panel], resulting in oxygen order with the wave vector $q = 1/3$ [31,43]. In this YBCO, we observed an oxygen-order peak at $\boldsymbol{Q}_{\text{OO}} = (-0.33,\ 0,\ l)$ under 300 K and $P = 0$ GPa [Fig. 1(c)]. Since CDW is also considered as an additional driving mechanism for understanding the T_c improvement under compression [17], we investigated CDW order in this YBCO. Figure 1(d) shows the short-ranged CDW order at $\boldsymbol{Q}_{\text{CDW}} = (-0.31,\ 0,\ l)$ at $T_c = 70$ K. These scattering observations are consistent with previous reports [31,34]. Note that the same CDW order in this doped YBCO was reported in hard x-ray scattering study under ambient pressure [32].

To explore the change in YBCO properties under high-pressure, hard x-ray diffraction measurement with 30-keV photon energy was performed on the same crystal. Figure 2(a) shows the scattering geometry (transmission configuration). As the volume of crystal unit cell shrinks under compression generally, we infer accordingly that the positions of the lattice Bragg peaks move to larger 2θ angle. As shown in Fig. 2(b), both 2θ angles of YBCO's in-plane Bragg peaks, (2, 0, 0) and (0, 2, 0), move toward the larger angles. Interestingly, the pressure-induced 2θ shifts of these (2, 0, 0) and (0, 2, 0) reflections are different. With increasing the HP, the shift of (2, 0, 0) is larger than that of (0, 2, 0) [Fig. 2(c), upper panel]. This indicates that the reduction of the lattice parameter along the a axis is greater than that along the b axis, increasing the orthorhombicity (b/a) of YBCO even with HP (i.e., isotropic pressure) [Fig. 2(c), lower panel].

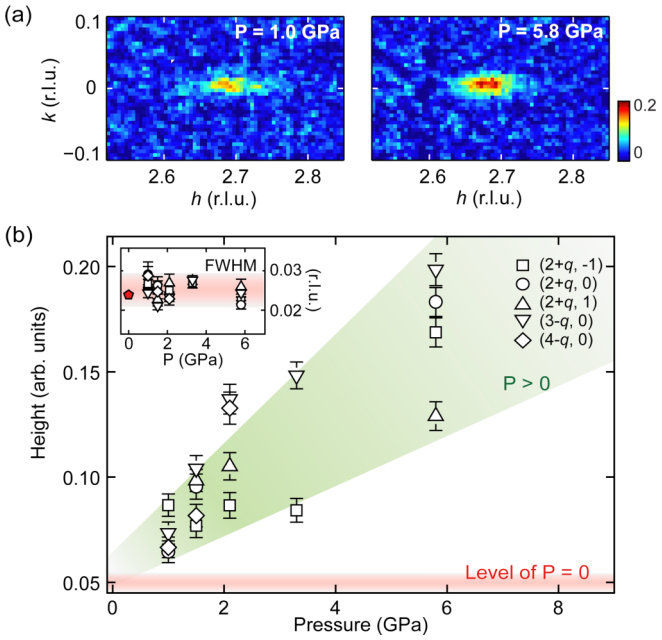

FIG. 3. (a) Experimental patterns of the oxygen order at $(h,k) = (3-q,\ 0)$ with $q = 0.33$ with 1.0 and 5.8 GPa. (b) Summary of fitting results on five oxygen-order peaks with varying pressure. The value of height is vertically shifted for comparison. Inset shows the full width at half maximum along the k direction. Note that the red-colored shading and data point at $P = 0$ (closed symbol) are estimated from the RSXS.

Under HP condition, the change in orthorhombicity brings our attention to exploring the oxygen order of YBCO. This is because, as shown in Fig. 1(b), the orthorhombic structure of YBCO is directly correlated with the Cu-O chain layer that has the intrinsic anisotropy (chain) feature. For this reason, we explored the oxygen order in YBCO to investigate whether it could be related to the increase in orthorhombicity under HP. Figure 3(a) shows the oxygen order patterns at $\boldsymbol{Q}_{\text{OO}} = (3-q,\ 0,\ l)$ at 1.0 and 5.8 GPa at room temperature. Note that the entire patterns are shown in Fig. 1(a). Due to the intrinsic quasi-2D feature of the oxygen order [44], the l value is rather insensitive to observe the oxygen order. Relatively, the intensity of the oxygen order peak (i.e., peak height) gets stronger at $P = 5.8$ GPa, while a change of the peak width (i.e., correlation length) along either the h or k direction is not obvious. For better statistics, we analyzed more oxygen-order peaks within our detectable windows, which are summarized in Fig. 3(b). Under HP condition, we could find the clear enhancement of the oxygen-order peaks' intensity compared with the zero-pressure level. Note that the absolute values of the peak height (y axis) have been shifted for comparison together and displayed in Fig. 3(b), because of their different geometric effects as well as the different scattering structure factor related with the corresponding nearest lattice Bragg peaks. From this result, we infer that the compression causes an oxygen redistribution inside the Cu-O chain layer. Moreover, as shown in the inset of Fig. 3(b), the width change is not clear, also inferring that a change in domain size of the oxygen order under HP is negligible in this experimental resolution.

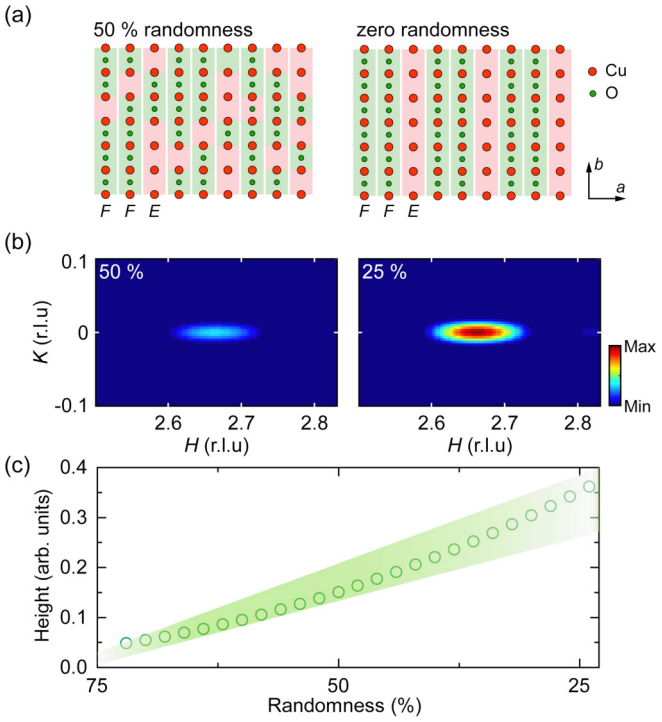

FIG. 4. (a) Modeled ortho-III structures with 50% (left) and 0% (right) randomness. (b) Simulated diffraction patterns of the ortho-III structures with 50% and 25% randomness. (c) Summary of the height of simulated oxygen-order peaks as a function of randomness.

In order to gain further insight into the changes in the oxygen order under HP, we simulated the diffraction patterns of the oxygen order in reciprocal space by varying the oxygen distribution in the Cu-O layer (i.e., real space). For this simulation, we employed 2D cell by 12 (a axis)×36 (b axis). Since the width change is not experimentally obvious in our resolution, we have constrained the fixed domain size (i.e., the finite cell size) for this simulation. Besides, to make simple ortho-III structure, oxygen atoms filled 2/3 of cell spaces and F-F-E-F-... chain patterns of oxygen distributions were generated along the a axis. The number of oxygen atoms in F and E chains was controlled by "randomness"—-defined by [(number of oxygen atoms in empty chains)/(2/3 × number of sites in all empty chains)]. For example, 50% randomness means that 1/3 of cell spaces in the empty chains are filled by the oxygen while the zero randomness indicates no oxygen in the empty chains—-i.e., the ideal ortho-III case [Fig. 4(a)]. In other words, this randomness is how much different from the ideal (i.e., perfect case) ortho-III structure in the Cu-O layer.

Figure 4(b) shows the simulated oxygen order diffraction patterns on two cases—-50% randomness (left panel) and 25% (right). As reducing the randomness (i.e., oxygen's locations are at the proper place), the pattern becomes strong and clear. Moreover, with varying the randomness, we could systematically trace the height of the oxygen-order peak [Fig. 4(c)]. Note that aiming for avoiding unrealistic cases [e.g., no oxygen order (i.e., 100% randomness) or ideal ortho-III structure], the oxygen-order patterns between 75% and 25% randomness have been tested. In this simulation, overall oxygen-order behaviors resemble the experimental observations in the oxygen

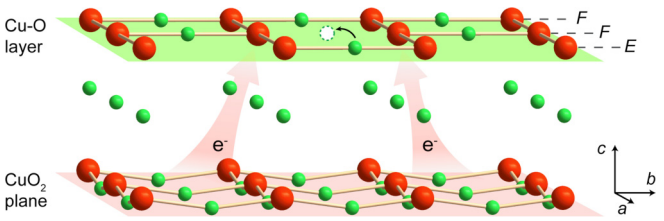

FIG. 5. Schematic drawing of charge transfer between Cu-O chain layer and CuO_2 plane upon HP. Curved black arrow represents the oxygen movement. The semitransparent arrows schematically represent the charge (electron) transfer from CuO_2 plane to Cu-O layer (i.e., hole doping of CuO_2 planes).

order under HP, as shown in Fig. 3(a). This analogy between the experiment and the simulation indicates that the randomness of oxygen distribution in the Cu-O chain layer is decreasing under HP. In this context, the reduced randomness by HP improves oxygen ordering, leading to the anisotropic stacking force in Cu-O layer (i.e., a bonding length change [46]), which would increase the orthorhombicity [47,48].

Furthermore, the oxygen rearrangement in the Cu-O chain under HP affects the charge configuration in the Cu-O chains, as well as a distance between Cu-O layer and CuO_2 plane [13]. Concurrently, the electronic structure (e.g., valence band) of Cu atoms can be varying, depending on whether Cu is adequately bonded with O or not [46,49]. Figure 5 shows a schematic diagram of Cu states' modification. While the oxygen rearrangement happens in the Cu-O chain, additional electrons transfer from the CuO_2 plane into the Cu-O chain layer to maintain the charge neutrality. Eventually, this HP effect causes an extra hole-doping effect in the CuO_2 plane, leading to an increase of T_c of underdoped $YBa_2Cu_3O_{6+x}$.

To understand the $T_c^{\max}|_{P>0}$ behavior in YBCO which is higher than $T_c^{\max}|_{P=0}$ [see Fig. 1(a) and corresponding text], however, in fact, this charge transfer may not be solely a reason. As we discussed in the Introduction, the natural interpretation is that decreased strength of the CDW order turns to increase T_c more. In this sense, we investigated a CDW under HP. Note that this YBCO shows the clear CDW under the ambient pressure [see Fig. 1(d)]. Figure 6(a) shows the diffraction patterns around $\boldsymbol{Q} = (3 + q^{\mathrm{CDW}}, 0, l)$ under $P = 1.0$ GPa (top panel: $T = 150$ K, middle: 70 K $\sim T_c$), where the q^{CDW} is around 0.31 r.l.u. (reciprocal lattice unit). Note that a scattering signal of CDW in $YBa_2Cu_3O_{6+x}$ is maximized around T_c [34]. While the oxygen order is clearly seen at both temperatures, no CDW signature has been seen in our detecting resolution. To confirm whether there is no signature, we also plot a difference (bottom panel) between two temperatures. It only shows a tiny residual signature of oxygen order. There are two possibilities (extrinsic and intrinsic) to explain this CDW absence. First, the extrinsic reason is that the generally weak CDW signal is buried by a high background signal from diamond in the DAC. Second, the intrinsic reason can be that the suppressed CDW is due to HP effect. Unfortunately, at this moment, we cannot distinguish them clearly. However, considering the recent inelastic x-ray scattering result [50], the suppression of CDW at even lower pressure is likely intrinsic. In addition, our results support that this behavior seems to be intrinsic.

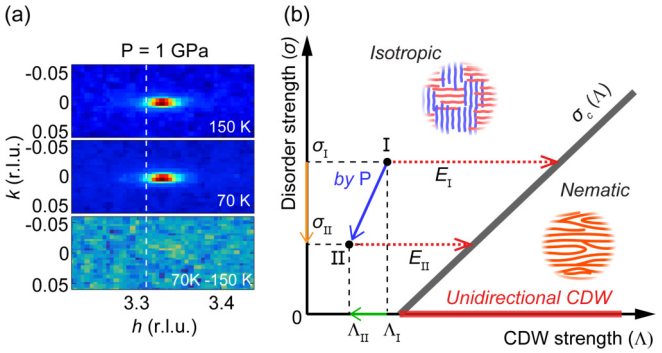

FIG. 6. (a) hk-diffraction pattern by 30-keV x ray under $P = 1.0$ GPa. The bottom panel is extracted by subtracting 150-K data (top) from 70-K data (middle). White dashed lines denote the CDW q position. (b) Schematic CDW phase diagram (more details in Ref. [39]). The green arrow along the CDW strength (Λ) axis and the orange arrow along the disorder strength (σ) axis indicate the directions of pressure effect. Blue and red (dotted) arrows denote total-pressure and magnetic-field effects, respectively. Note that state I and state II denote the ambient and compressed YBCO states, respectively.

Since the fact that the modified structural disorder in the Cu-O layer (i.e., oxygen rearrangement) affects the charge distribution (i.e., charge-density potential) in the CuO_2 plane, the quenched disorder in the CuO_2 plane, which originates from the charge potential of defects [37], is correspondingly modified through the pressure. This circumstance may reduce the pinning centers for CDW fluctuation in the CuO_2 plane [36], suppressing the disorder-pinned CDW fluctuation, which is consistent with the theoretical predictions [33,37,38]. As a consequence, we come to an answer to the initial question we posed. There are two factors contributing to the compression-induced T_c change. Firstly, in agreement with the previous works [14,20–23], high pressure promoted the charge transfer (i.e., hole doping into the CuO_2 plane) leads to the increment in T_c. Secondly, the quenched disorder state is modified, resulting in the suppression of the CDW. Subsequently, due to the competing nature between YBCO's superconductivity and CDW [29–39], $T_c^{\max}|_{P>0}$, which is even higher than the optimal T_c at ambient pressure, can be achieved through compression.

Finally, we try to extend these results to reconcile the broader context of CDW phenomena in underdoped $YBa_2Cu_3O_{6+x}$ [see Fig. 6(b)]. Considering theoretical predictions [51] and corresponding experimental results [39], the ideal CDW state (i.e., ground state) in YBCO is of long-range, anisotropic (or nematic) ordering when superconductivity is suppressed by the external magnetic field (H field). Theoretically, this nematic order also prefers structural nematicity (i.e., orthorhombicity) [37]. By enhancing $YBa_2Cu_3O_{6+x}$'s orthorhombicity under hydrostatic pressure, it would become easier to develop nematic order in compressed YBCO [state II, labeled in Fig. 6(b)] compared to ambient pressure YBCO (state I). On the other hand, the oxygen redistribution in the Cu-O layer under high pressure suppresses the disorder-pinned CDW fluctuating portion. Therefore, we infer that a pressure condition causes a decrease in the disorder strength (σ) [37,39,51] in the CuO_2 plane, which is reasonably proportional to or dominated by the quantity of the structural disorders in the Cu-O chain layer [36,52]. Ultimately, the energy cost for developing the nematic order at state II (E_{II}, i.e., H-field strength) can be smaller than that at state I (E_I) [39], which is well supported by our findings (i.e., $\sigma_{II} < \sigma_I$ and $\Lambda_{II} < \Lambda_I$).

IV. SUMMARY

In summary, we present the detailed study of structural disorder in YBCO using x-ray scattering under high pressure. We observed the enhanced oxygen order under hydrostatic pressure, resulting in the broken quenched disorder state and the decreased disorder which leads to changes in the hole doping as well as the weakening of the CDW fluctuation. These findings suggest the underlying mechanism of the pressure-induced T_c change in YBCO. Simultaneously, the pressure-induced clean nature (i.e., suppressed disorder) could be favorable to the development of nematic order in YBCO. This potential development suggests that there is a pressure threshold above which further compression has limited influence on T_c.

ACKNOWLEDGMENTS

We thank Laimei Nie and Steven A. Kivelson for valuable discussions and comments. Soft x-ray experiments were carried out at the SSRL, SLAC National Accelerator Laboratory, supported by the U.S. Department of Energy, Office of Science, Office of Basic Energy Sciences under Contract No. DE-AC02-76SF00515. W.M. and Y.L. acknowledge support by the U.S. Department of Energy, Office of Basic Energy Sciences, Materials Sciences and Engineering Division, under Contract No. DE-AC02-76SF00515. H.H. acknowledges support of China Scholarship Council. J.S.S., C.K.B., and G.S. acknowledge support of DOE-MSED under Award No. DE-FG02-99ER45775. High-pressure studies were performed at HPCAT (Sector 16), APS, Argonne National Laboratory. HPCAT operations are supported by DOE-NNSA under Award No. DE-NA0001974, with partial instrumentation funding by NSF. The Advanced Photon Source is a U.S. Department of Energy Office of Science User Facility operated for the Department of Energy, Office of Science by Argonne National Laboratory under Contract No. DE-AC02-06CH11357. M.F. and T. N. are supported by Grant-in-Aid for Scientific Research (A) (Grant No. 16H02125) and for Scientific Research (C) (Grant No. 16K05460), respectively.

[1] J. G. Bednorz and K. A. Müller, Possible high T_c superconductivity in the Ba−La−Cu−O system, Z. Phys. B **64**, 189 (1986).

[2] M. K. Wu, J. R. Ashburn, C. J. Torng, P. H. Hor, R. L. Meng, L. Gao, Z. J. Huang, Y. Q. Wang, and C. W. Chu, Superconductivity

at 93 K in a New Mixed-Phase Y-Ba-Cu-O Compound System At Ambient Pressure, Phys. Rev. Lett. **58**, 908 (1987).

[3] Z. Z. Sheng and A. M. Hermann, Superconductivity in the rare-earth-free Tl–Ba–Cu–O system above liquid-nitrogen temperature, Nature (London) **332**, 55 (1988).

[4] P. A. Lee, N. Nagaosa, and X. G. Wen, Doping a Mott insulator: Physics of high-temperature superconductivity, Rev. Mod. Phys. **78**, 17 (2006).

[5] B. Keimer, S. A. Kivelson, M. R. Norman, S. Uchida, and J. Zaanen, From quantum matter to high-temperature superconductivity in copper oxides, Nature (London) **518**, 179 (2015).

[6] A. Schilling, M. Cantoni, J. D. Guo, and H. R. Ott, Superconductivity above 130 K in the Hg–Ba–Ca–Cu–O system, Nature (London) **363**, 56 (1993).

[7] A. P. Drozdov, M. I. Eremets, I. A. Troyan, V. Ksenofontov, and S. I. Shylin, Conventional superconductivity at 203 Kelvin at high pressures in the sulfur hydride system, Nature (London) **525**, 73 (2015).

[8] C. W. Chu, P. H. Hor, R. L. Meng, L. Gao, Z. J. Huang, and Y. Q. Wang, Evidence for Superconductivity Above 40 K in the La-Ba-Cu-O Compound System, Phys. Rev. Lett. **58**, 405 (1987).

[9] C. W. Chu, L. Gao, F. Chen, Z. J. Huang, R. L. Meng, and Y. Y. Xue, Superconductivity above 150 K in $HgBa_2Ca_2Cu_3O_{8+\delta}$ at high pressures, Nature (London) **365**, 323 (1993).

[10] S. M. Souliou, A. Subedi, Y. T. Song, C. T. Lin, K. Syassen, B. Keimer, and M. Le Tacon, Pressure-induced phase transition and superconductivity in $YBa_2Cu_4O_8$, Phys. Rev. B **90**, 140501 (2014).

[11] P. L. Alireza, G. H. Zhang, W. Guo, J. Porras, T. Loew, Y.-T. Hsu, G. G. Lonzarich, M. Le Tacon, B. Keimer, and S. E. Sebastian, Accessing the entire overdoped regime in pristine $YBa_2Cu_3O_{6+x}$ by application of pressure, Phys. Rev. B **95**, 100505(R) (2017).

[12] S. Sadewasser, J. S. Schilling, A. P. Paulikas, and B. W. Veal, Pressure dependence of T_c to 17 GPa with and without relaxation effects in superconducting $YBa_2Cu_3O_x$, Phys. Rev. B **61**, 741 (2000).

[13] J. Jorgensen, S. Pei, P. Lightfoot, D. Hinks, B. Veal, B. Dabrowski, A. Paulikas, R. Kleb, and I. Brown, Pressure-induced charge transfer and dT_c/dP in $YBa_2Cu_3O_{7-x}$, Physica C **171**, 93 (1990).

[14] C. Almasan, S. Han, B. Lee, L. Paulius, M. Maple, B. Veal, J. Downey, A. Paulikas, Z. Fisk, and J. Schirber, Pressure Dependence of T_c and Charge Transfer in $YBa_2Cu_3O_x$ ($6.35 \leqslant x \leqslant 7$) Single Crystals, Phys. Rev. Lett. **69**, 680 (1992).

[15] J. Metzger, T. Weber, W. Fietz, K. Grube, H. Ludwig, T. Wolf, and H. Wühl, Separation of the intrinsic pressure effect on T_c of $YBa_2Cu_3O_{6.7}$ from a T_c enhancement caused by pressure-induced oxygen ordering, Physica C **214**, 371 (1993).

[16] S. Sadewasser, Y. Wang, J. S. Schilling, H. Zheng, A. P. Paulikas, and B. W. Veal, Pressure-dependent oxygen ordering in strongly underdoped $YBa_2Cu_3O_{7-y}$, Phys. Rev. B **56**, 14168 (1997).

[17] O. Cyr-Choinière, D. LeBoeuf, S. Badoux, S. Dufour-Beausejour, D. A. Bonn, W. N. Hardy, R. Liang, N. Doiron-Leyraud, and L. Taillefer, Suppression of charge order by pressure in the cuprate superconductor $YBa_2Cu_3O_y$: Restoring the full superconducting dome, arXiv:1503.02033.

[18] T. Tomita, J. S. Schilling, L. Chen, B. W. Veal, and H. Claus, Enhancement of the Critical Current Density of $YBa_2Cu_3O_x$ Superconductors Under Hydrostatic Pressure, Phys. Rev. Lett. **96**, 077001 (2006).

[19] W. E. Pickett, Effect of uniaxial strains on the electronic structure of $YBa_2Cu_3O_7$, Physica C **289**, 51 (1997).

[20] J. J. Neumeier and H. A. Zimmermann, Pressure dependence of the superconducting transition temperature of $YBa_2Cu_3O_7$ as a function of carrier concentration: A test for a simple charge-transfer model, Phys. Rev. B **47**, 8385 (1993).

[21] R. P. Gupta and M. Gupta, Relationship between pressure-induced charge transfer and the superconducting transition temperature in $YBa_2Cu_3O_{7-\delta}$ superconductors, Phys. Rev. B **51**, 11760 (1995).

[22] X. J. Chen, H. Q. Lin, and C. D. Gong, Pressure Dependence of T_c in Y-Ba-Cu-O Superconductors, Phys. Rev. Lett. **85**, 2180 (2000).

[23] P. Gao, R. Zhang, and X. Wang, Pressure induced self-doping and dependence of critical temperature in stoichiometry $YBa_2Cu_3O_{6.95}$ predicted by first-principle and BVS calculations, AIP Adv. **7**, 035215 (2017).

[24] H. Alloul, J. Bobroff, M. Gabay, and P. J. Hirschfeld, Defects in correlated metals and superconductors, Rev. Mod. Phys. **81**, 45 (2009).

[25] F. Coneri, S. Sanna, K. Zheng, J. Lord, and R. De Renzi, Magnetic states of lightly hole-doped cuprates in the clean limit as seen via zero-field muon spin spectroscopy, Phys. Rev. B **81**, 104507 (2010).

[26] G. Grissonnanche, O. Cyr-Choiniere, F. Laliberté, S. R. De Cotret, A. Juneau-Fecteau, S. Dufour-Beauséjour, M.-E. Delage, D. LeBoeuf, J. Chang, and B. Ramshaw, Direct measurement of the upper critical field in cuprate superconductors, Nat. Commun. **5**, 3280 (2014).

[27] R. Liang, D. A. Bonn, and W. N. Hardy, Evaluation of CuO_2 plane hole doping in $YBa_2Cu_3O_{6+x}$ single crystals, Phys. Rev. B **73**, 180505 (2006).

[28] S. I. Schlachter, W. H. Fietz, K. Grube, Th. Wolf, B. Obst, P. Schweiss, and M. Kläser, The effect of chemical doping and hydrostatic pressure on T_c of $Y_{1-y}Ca_yBa_2Cu_3O_x$ single crystals, Physica C **328**, 1 (1999).

[29] G. Ghiringhelli, M. Le Tacon, M. Minola, S. Blanco-Canosa, C. Mazzoli, N. B. Brookes, G. M. De Luca, A. Frano, D. G. Hawthorn, F. He, T. Loew, M. Moretti Sala, D. C. Peets, M. Salluzzo, E. Schierle, R. Sutarto, G. A. Sawatzky, E. Weschke, B. Keimer, and L. Braicovich, Long-range incommensurate charge fluctuations in $(Y,Nd)Ba_2Cu_3O_{6+x}$, Science **337**, 821 (2012).

[30] J. Chang, E. Blackburn, A. T. Holmes, N. B. Christensen, J. Larsen, J. Mesot, R. Liang, D. A. Bonn, W. N. Hardy, A. Watenphul, M. v. Zimmermann, E. M. Forgan, and S. M. Hayden, Direct observation of competition between superconductivity and charge density wave order in $YBa_2Cu_3O_{6.67}$, Nat. Phys. **8**, 871 (2012).

[31] A. J. Achkar, R. Sutarto, X. Mao, F. He, A. Frano, S. Blanco-Canosa, M. Le Tacon, G. Ghiringhelli, L. Braicovich, M. Minola, M. M. Sala, C. Mazzoli, R. Liang, D. A. Bonn, W. N. Hardy, B. Keimer, G. A. Sawatzky, and D. G. Hawthorn, Distinct Charge Orders in the Planes and Chains of Ortho-III-Ordered $YBa_2Cu_3O_{6+\delta}$ Superconductors Identified by Resonant Elastic X-Ray Scattering, Phys. Rev. Lett. **109**, 167001 (2012).

[32] E. Blackburn, J. Chang, M. Hücker, A. T. Holmes, N. B. Christensen, R. Liang, D. A. Bonn, W. N. Hardy, U. Rütt, O. Gutowski, M. v. Zimmermann, E. M. Forgan, and S. M. Hayden, X-ray Diffraction Observations of a Charge-Density-Wave Order in Superconducting Ortho-II $YBa_2Cu_3O_{6.54}$ Single Crystals in Zero Magnetic Field, Phys. Rev. Lett. **110**, 137004 (2013).

[33] L. E. Hayward, D. G. Hawthorn, R. G. Melko, and S. Sachdev, Angular fluctuations of a multicomponent order describe the pseudogap of $YBa_2Cu_3O_{6+x}$, Science **343**, 1336 (2014).

[34] S. Blanco-Canosa, A. Frano, E. Schierle, J. Porras, T. Loew, M. Minola, M. Bluschke, E. Weschke, B. Keimer, and M. Le Tacon, Resonant x-ray scattering study of charge-density wave correlations in $YBa_2Cu_3O_{6+x}$, Phys. Rev. B **90**, 054513 (2014).

[35] S. Gerber, H. Jang, H. Nojiri, S. Matsuzawa, H. Yasumura, D. A. Bonn, R. Liang, W. N. Hardy, Z. Islam, A. Mehta, S. Song, M. Sikorski, D. Stefanescu, Y. Feng, S. A. Kivelson, T. P. Devereaux, Z.-X. Shen, C.-C. Kao, W.-S. Lee, D. Zhu, and J.-S. Lee, Three-dimensional charge density wave order in $YBa_2Cu_3O_{6.67}$ at high magnetic fields, Science **350**, 949 (2015).

[36] T. Wu, H. Mayaffre, S. Kramer, M. Horvatic, C. Berthier, W. N. Hardy, R. Liang, D. A. Bonn, and M. H. Julien, Incipient charge order observed by NMR in the normal state of $YBa_2Cu_3O_y$, Nat. Commun. **6**, 6438 (2015).

[37] L. Nie, L. E. H. Sierens, R. G. Melko, S. Sachdev, and S. A. Kivelson, Fluctuating orders and quenched randomness in the cuprates, Phys. Rev. B **92**, 174505 (2015).

[38] Y. Caplan, G. Wachtel, and D. Orgad, Long-range order and pinning of charge-density waves in competition with superconductivity, Phys. Rev. B **92**, 224504 (2015).

[39] H. Jang, W.-S. Lee, H. Nojiri, S. Matsuzawa, H. Yasumura, L. Nie, A. V. Maharaj, S. Gerber, Y. J. Liu, A. Mehta, D. A. Bonn, R. Liang, W. N. Hardy, C. A. Burns, Z. Islam, S. Song, J. Hastings, T. P. Devereaux, Z. X. Shen, S. A. Kivelson, C.-C. Kao, D. Zhu, and J.-S. Lee, Ideal charge-density-wave order in the high-field state of superconducting YBCO, Proc. Nat. Acad. Sci. USA **113**, 14645 (2016).

[40] M. Eschrig, The effect of collective spin-1 excitations on electronic spectra in high-T_c superconductors, Adv. Phys. **55**, 47 (2007).

[41] M. Le Tacon, G. Ghiringhelli, J. Chaloupka, M. Moretti Sala, V. Hinkov, M. W. Haverkort, M. Minola, M. Bakr, K. J. Zhou, S. Blanco-Canosa, C. Monney, Y. T. Song, G. L. Sun, C. T. Lin, G. M. De Luca, M. Salluzzo, G. Khaliullin, T. Schmitt, L. Braicovich, and B. Keimer, Intense paramagnon excitations in a large family of high-temperature superconductors, Nat. Phys. **7**, 725 (2011).

[42] T. Naito, T. Nishizaki, Y. Watanabe, and N. Kobayashi, *Advances in Superconductivity IX* (Springer-Verlag, Tokyo, 1997), p. 601.

[43] K. Shibata, T. Nishizaki, T. Naito, M. Maki, and N. Kobayashi, Superconducting properties of untwinned $YBa_2Cu_3O_y$ single crystals annealed in high-pressure oxygen, Physica B **284-288**, 1027 (2000).

[44] M. v. Zimmermann, J. R. Schneider, T. Frello, N. H. Andersen, J. Madsen, M. Käll, H. F. Poulsen, R. Liang, P. Dosanjh, and W. N. Hardy, Oxygen-ordering superstructures in underdoped $YBa_2Cu_3O_{6+x}$ studied by hard x-ray diffraction, Phys. Rev. B **68**, 104515 (2003).

[45] G. Shen and H. K. Mao, High-pressure studies with x-rays using diamond anvil cells, Prog. Phys. **80**, 016101 (2017).

[46] E. S. Božin, A. Huq, B. Shen, H. Claus, W. K. Kwok, and J. M. Tranquada, Charge-screening role of c-axis atomic displacements in $YBa_2Cu_3O_{6+x}$ and related superconductors, Phys. Rev. B **93**, 054523 (2016).

[47] J. Jorgensen, S. Pei, P. Lightfoor, H. Shi, A. Paulikas, and B. Veal, Time-dependent structural phenomena at room temperature in quenched $YBa_2Cu_3O_{6.41}$: Local oxygen ordering and superconductivity, Physica C **167**, 571 (1990).

[48] B. W. Veal, H. You, A. P. Paulikas, H. Shi, Y. Fang, and J. W. Downey, Time-dependent superconducting behavior of oxygen-deficient $YBa_2Cu_3O_x$: Possible annealing of oxygen vacancies at 300 K, Phys. Rev. B **42**, 4770 (1990).

[49] V. M. Matic and N. D. Lazarov, Impact of chain fragmentation on charge transfer scenario and two-plateaus-like behavior of T_c (x) in $YBa_2Cu_3O_{6+x}$, Solid State Commun. **142**, 165 (2007).

[50] S. M. Souliou, H. Gretarsson, G. Garbarino, A. Bosak, J. Porras, T. Loew, B. Keimer, and M. Le Tacon, Rapid suppression of the charge density wave in $YBa_2Cu_3O_{6.6}$ under hydrostatic pressure, Phys. Rev. B **97**, 020503(R) (2018).

[51] L. Nie, G. Tarjus, and S. A. Kivelson, Quenched disorder and vestigial nematicity in the pseudogap regime of the cuprates, Proc. Nat. Acad. Sci. USA **111**, 7980 (2014).

[52] J. Bobowski, J. Baglo, J. Day, L. Semple, P. Dosanjh, P. Turner, R. Harris, R. Liang, D. Bonn, and W. Hardy, Oxygen chain disorder as the weak scattering source in $YBa_2Cu_3O_{6.50}$, Phys. Rev. B **82**, 134526 (2010).